ISSN 2229-5518

Modeling and Simulation of High-Performance Symmetrical Linear Actuator

Juma Yousuf Alaydi

ABSTRACT

In this paper the dynamic performance analysis of servovalve controlling symmetrical linear actuator was investigated. Hydraulic actuators are characterized by their ability to impart large forces at high speeds and are used in many industrial motion systems. In this application the good dynamic performance is important thus the analyzed actuator was included in a servo loop comprising a feedback transducer and electronic controller. This research paper may assist the majority of electronic servo-controllers accompanied with analogue based implementations of the well-known PID controller. However, the requirement to implement advanced control strategies has led to an increased interest in the use of digital signal processors (DSPs) in this field. One design approach which merits special consideration is the use of computer simulation software to model the hydraulic plant and electronic servo-controller, and to generate and test embedded code for the target digital signal processors (DSPs), this paper discusses some of the issues involved in controlling linear hydraulic actuators. The analysis of the hydraulic control system presented is supported by experimental data and explains the extremely high level of performance.
The results of this paper, being physically structured linear dynamic models of the hydraulic servo-system, which are sufficiently simplified to allow identification of the model parameters from experimental data, as well as experimental validation of the quality of the models.

KEY WORDS: Electrohydraulic servovalves, linear actuator, dynamic performance, linear dynamic models

1. INTRODUCTION

The range of applications for electro-hydraulic servo systems is diverse, and includes manufacturing systems, materials test machines, active suspension systems, mining machinery, fatigue testing, flight simulation, paper machines, ships and electromagnetic marine engineering, injection molding machines, robotics, and steel and aluminum mill equipment. Although electrical motors are sometimes used in many of these applications, motion control systems requiring either very high force or wide bandwidth are often addressed more efficiently with electrohydraulic rather than electromagnetic means. In general, applications with bandwidths of greater than about 20 Hz or control power greater than about 15 kW may be regarded as suitable for servo-hydraulic techniques [1]. Apart from the ability to deliver higher forces at fast speeds, servo-hydraulic systems offer several other benefits over their electrical counterparts. For example, hydraulic systems are mechanically stiffer, resulting in higher machine frame resonant frequencies for a given power level, higher loop gain and improved dynamic performance.

- *Dr. Juma Yousuf Alaydi is an Associated Professor in Mechanical Engineering and Mechatronics in the Islamic University of Gaza - Palestine. E-mail: jalaydi@iugaza.edu*

Unfortunately hydraulic systems also exhibit several inherent non-linear effects which can complicate the control problem. The vast majority of electronic closed loop controllers are based on simple analogue circuit designs offering robust, low cost implementations of the well known PID control strategy [2]. This approach works well in systems with simple topology and limited bandwidth. However the growing use of complex control strategies, coupled with the need to support enhanced features such as data-logging and digital communications, has led to increased interest in the use of digital processors for control of hydraulic servo-systems. Nowhere is this more apparent than in the field of mechanical test equipment, where the use of a programmable digital processor allows the same servo controller to be used with a wide range of hydraulic systems.
The most widespread method for electromagnetic field modeling of linear actuators is the finite element method in its different formulations [3]-[10]. Two principal approaches are possible to solve the problem coupled and decoupled. The coupled approach in [3] requires solution of all the problems simultaneously. The decoupled model in [2] involves separate solutions of the magnetostatic field problem, where a set of solutions is obtained for a wide range of current and displacement, and of the electric circuit and mechanical motion problems. The main drawback of the decoupled model is that the eddy currents are not taken into account. Solution of the dynamics for different types of actuators is presented in [4], [5], and [7-

15]. The theoretical modeling of hydraulic actuators is well-developed in the past decades. Standard text-books on hydraulic servo-systems, as for instance those by Merrit [6] and by DeRose [8], provide a thorough analysis of the basics of the hydraulic servo technique.

This paper reviews some of the issues facing the hydraulic control engineer and discusses the suitability of high-speed digital signal processors (DSPs) for control of servo-hydraulic systems. The application report begins with an evaluation of the (DSP) for use in electro-hydraulic servo-controllers of (DSP) platform optimized for digital control applications. The principal components of the hydraulic system were described. Mathematical models for the various plant elements were developed using Simulink. A case study of a hydraulic control system and deals with fitting real data to the model to validate its behavior was presented. The application report concludes with a brief summary and discussion of the application and design process.

The performance of a high quality hydraulic actuator is very dependent on the servo-controller. In this paper modeling and simulation of high-performance symmetrical linear actuator sufficiently simplified to allow identification of the model parameters from experimental data, as well as experimental validation of the quality of the models to assist researchers in the field of hydraulic power system.

2. DESCRIPTION OF HYDRAULIC SYSTEM

A typical position controlled hydraulic system consists of a power supply, flow control valve, linear actuator, displacement transducer, and electronic servo-controller as shown in Fig. 1 and Fig. 2. The servo controller compares the signal from the feedback displacement transducer with an input demand to determine the position error, and produces a command signal to drive the flow control valve. The control valve adjusts the flow of pressurized oil to move the actuator until the desired position is attained: a condition indicated by the error signal falling to zero. A force controlled hydraulic system operates in a similar way, except that the oil flow is adjusted to achieve an output force, measured by a suitable transducer.

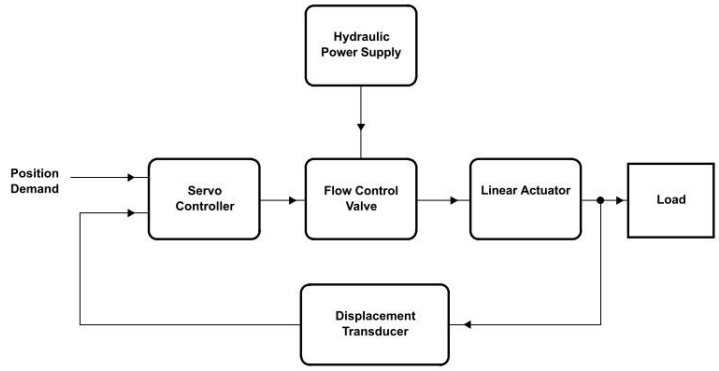

Fig. 1. Block diagram of a position controlled hydraulic servo system

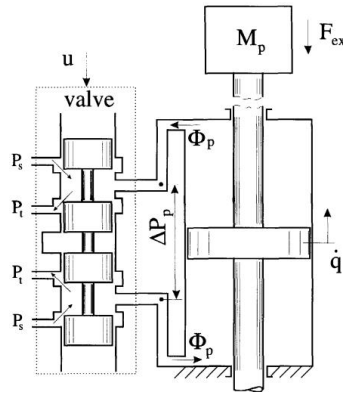

Fig. 2. Schematic drawing of hydraulic servo-system

High pressure systems suffer from more leakage, but have better dynamic performance and are both smaller and lighter: significant advantages in mobile and aircraft applications. In many high performance systems 210 bar is a standard choice of system pressure. Oil is drawn from a reservoir (tank) into a rotary vane or piston pump, driven at constant speed by an electric motor. The oil is driven at constant flow rate into an adjustable pressure relief valve, which regulates system pressure by allowing excess oil to return to the reservoir once a pre-defined pressure threshold has been reached. Pressurized hydraulic oil is carried to the servo-valve through a system of rigid or flexible piping, possibly fitted with electrically operated shut-off valves to control hydraulic start-up and shut-down sequences. Oil is returned from the valve to the tank through a low pressure return pipe, which is often fitted with an in-line heat exchanger for temperature regulation of the oil.

2.1 FLOW CONTROL VALUE

The electro-hydraulic flow control valve acts as a high gain electrical to hydraulic transducer, the input to which is an electrical voltage or current, and the output a variable flow of oil. The valve consists of a spool with lands machined into it, moving within a cylindrical sleeve. The lands are aligned with apertures cut in the sleeve such that movement of the spool progressively changes the exposed aperture size and alters differential oil flow between two control ports.

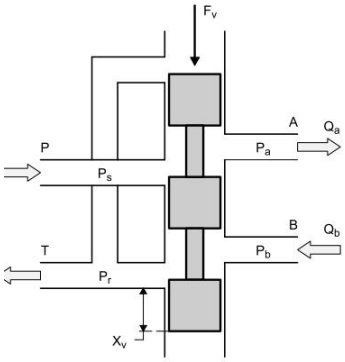

Fig. 3. Three Land, Four-way Flow Control Valve Spool

Fig. 3 shows the spool configuration of a typical 3-4 flow control valve. The ports are labeled P (pressure), T (tank), and A and B (load control ports). The spool is shown displaced a small distance (xv) as a result of a command force applied to one end, and arrows at each port indicate the direction of fluid flow which results. With no command force applied (Fv = 0), the spool is centralized and all ports are closed off by the lands resulting in no load flow.

In the context of hydraulic servo-systems, flow control valves fall broadly into two main categories:

- Proportional valves and servo-valves.
- Proportional valves use direct actuation of the spool from an electrical solenoid or torque motor.

Whereas servo-valves use at least one intermediate hydraulic amplifier stage between the electrical torque motor and the spool. A major advantage of proportional valves is that they are largely unaffected by changes in supply pressure and oil viscosity. However, the relatively large armature mass and large time constant associated with the coil means that these valves generally have poorer dynamic performance compared with servo-valves of equivalent flow characteristics.

The basic servo-valve produces a control flow proportional to input current for a constant load. While the dynamic performance of a servo-valve is influenced somewhat by operating conditions as supply pressure, input signal level, fluid and ambient temperature and so on.

Two stage servo-valves may be further divided into nozzle-flapper and jet pipe types. Both use a similar design of electromagnetic torque motor, but the hydraulic amplifier circuits are radically different. Nozzle-flapper type servo-valves are currently by far the most common in high performance servo applications and the description which follows is based on this type of valve.

A typical nozzle-flapper type servo-valve is shown in Fig. 4. High pressure hydraulic oil is supplied at the inlet pressure port (P), and a low pressure return line to the oil reservoir is connected to the tank port (T). The two hydraulic control ports (A and B) carry the control oil flows to and from the load actuator

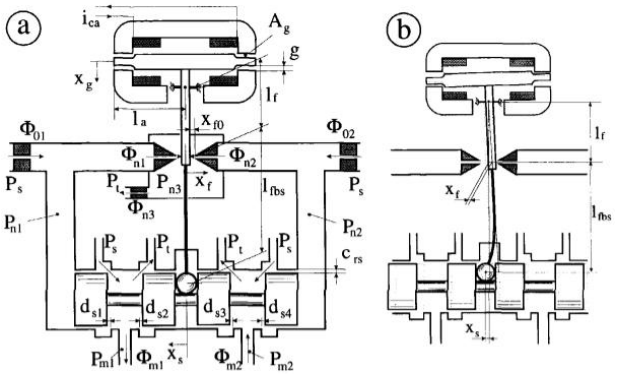

Fig. 4. Nozzle-flapper Type Servo-valve

2.2 LINEAR HYDRAULIC ACTUATOR

A hydraulic actuator is a device which converts hydraulic energy into mechanical force or motion. Actuators may be divided into those with linear movement, and those with rotary movement. Linear actuators may be further sub-divided into those in which hydraulic pressure is applied to one side of the piston only single acting, and are capable of movement only in one direction, and those in which pressure is applied to both sides of the piston double acting, and are therefore capable of controlled movement in both directions.

The description which follows is based on a linear, double-acting, double-ended actuator. A cross section of such an actuator is shown in Fig. 5. The actuator consists of a rod and central annulus, and incorporates low friction seals fitted to the piston annulus and at each of the cylinder end caps to minimize leakage. Control ports are drilled into each end of the cylinder to allow hydraulic fluid to flow in and out of the two chambers.

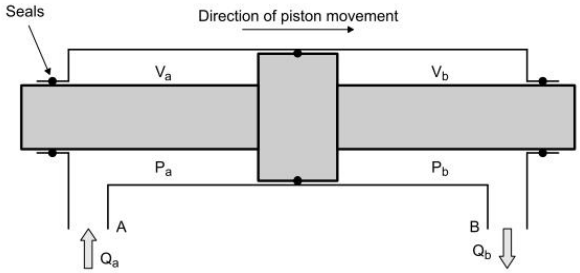

Fig. 5. Cross-sectional Diagram of Double-ended, Double-acting Linear Actuator

The position of the piston is determined by the hydraulic fluid pressures in the chambers on either side of the central annulus, and may be adjusted by forcing fluid into one control port while allowing it to escape from the other. In the diagram above, hydraulic fluid is shown entering control port A while escaping from port B. This causes an increase in fluid pressure in the chamber to the left of the piston annulus, and a decrease in pressure in the right chamber. The net pressure difference exerts a force on the active area of the annulus which moves the piston to the right as shown. Adjustment of piston position is therefore a matter of controlling the differential oil flow between the two actuator control ports.

2.3 DISPLACEMENT TRANSDUCER

Position transducers are usually collocated with the actuator, and often attached directly to the piston rod. Various types of feedback transducer are in use, including incremental or absolute encoders, inductive linear variable differential transformer (LVDT's) and rotary variable differential transformer (RVDT's), linear and rotary potentiometers, and resolvers. In industrial applications employing linear displacement control, the LVDT is a common choice of feedback transducer due to its accuracy and robustness. The transducer is usually selected such that its bandwidth is ten times or so higher than that of the servo-valve and actuator, and is often omitted from a first analysis of the system.

2.4 SERVO CONTROLLER

Fig. 6 shows the layout of the servo-controller block.

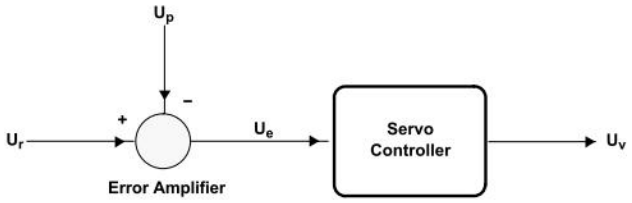

Fig. 6. Block Diagram of the Analogue Controller

The error amplifier continuously monitors the input reference signal Ur and compares it against the actuator position U_p measured by a displacement transducer to yield an error signal U_e as shown in "(1)".

$$U_e = U_r - U_p \quad (1)$$

The error is manipulated by the servo controller according to a pre-defined control law to generate a command signal u_v to drive the hydraulic flow control valve. Most conventional electro-hydraulic servo-systems use a PID form of control, occasionally enhanced with velocity feedback. The processing of the error signal in such a controller is a function of the proportional, integral, and derivative gain compensation settings according to the control law shown in "(2)".

$$u_v(t) = K_p u_e(t) + K_i \int u_e dt + K_d \frac{du_e}{dt} \quad (2)$$

where K_p, K_i, and K_d are the PID constants, ue is the error signal and uv is the controller output [16],[17], and [19].

3 HYDRAULIC SYSTEM MODELING

This section develops basic mathematical models of the hydraulic components described before, and makes use of Simulink modeling software from The Mathwork Inc. For further information on this software, the reader is referred to the references at the end of this application report to the training courses run by The Mathworks Inc. Examples of graphical models of some of the major hydraulic elements are shown in the case study below.

3.1 FLOW CONTROL SERVO-VALVE

These servovalves combine the functions of pressure and flow control to provide characteristics which contribute effective damping in highly-resonant loaded servo systems. Flow from these servovalves is determined not only by the electrical input signal, but also by the differential load pressure. For a linear transfer function approximation to dynamic response, it may again be assumed that principles of superposition prevail. With this assumption, flow from the servovalve may be considered separately dependent upon input current and load pressure.

For most pressure-flow servovalves, the dynamic response of each flow relationship of low to current, and flow to load pressure can be approximated by a critically damped, second order transfer function. In addition, it has been found experimentally that these dynamic responses are nearly equal. The assumption of identical dynamics further simplifies the overall transfer function, so that the dynamic performance expressed mathematically in "(3)".

$$Q(s) = (k_l\, i - k_2\, p)\left(\frac{1}{1+\frac{s}{w_n}}\right)^2 \quad (3)$$

k_l servovalve sensitivity to input current
k_2 servovalve sensitivity to load pressure
w_n equivalent servovalve natural frequency critical damped

3.1.1 TORQUE MOTOR

For simplicity, the electrical characteristics of the servo-valve torque motor may be modeled as a series L-R circuit, neglecting for the time being any back-EMF effects generated by the load. The transfer function of a series L-R circuit is shown in "(4)".

$$\frac{I(s)}{V(s)} = \frac{1}{sL_c+R_c} \quad (4)$$

Where L_c is the inductance of the motor coil, and Rc the combined resistance of the motor coil and the current sense resistor of the servo amplifier. Values of inductance and resistance for series and parallel winding configurations of the motor are published in the manufacturer's data sheet. The lateral force on the valve spool is proportional to torque motor current, but oil flow rate at the control ports also depends upon the pressure drop across the load.

3.1.2 VALVE SPOOL DYNAMICS

A servo-valve is a complex device which exhibits a high-order non-linear response, and knowledge of a large number of internal valve parameters is required to formulate an accurate mathematical model. Indeed, any parameters such as nozzle and orifice sizes, spring rates, spool geometry and so on, are adjusted by the manufacturer to tune the valve response and are not normally available to the user. Practically all physical systems exhibit some non-linearity: in the simplest case this may be a physical limit of movement, or it may arise from the effects of friction, hysteresis, mechanical wear or backlash. When modeling complex servo-valves, it is sometimes possible to ignore any inherent non-linearity and employ a small perturbation analysis to derive a linear model which approximates the physical system. Such models are often based on classical first or second order differential equations, the coefficients of which are chosen to match the response of the valve based on frequency plots taken from the data sheet.

A simple first or second order model yields only an approximation to actual behavior, however the servo-valve is not the primary dynamic element in a typical hydraulic servo system and is generally selected such that the frequency of the 90 degree phase point is a factor of at least three higher than that of the actuator. For this reason it is usually only necessary to accurately model valve response through a relatively low range of frequencies, and the servo-valve dynamics may be approximated by a second order transfer function without serious loss of accuracy.

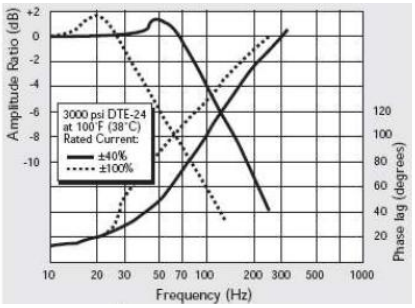

Fig. 7. Typical Servo-valve Frequency Response Curve

A typical performance graph for a high-response servo-valve is shown in Fig. 7 [2]. Assuming a second order approximation is to be used, suitable values for natural frequency and damping ratio will need to be determined from the graph. Natural frequency ω_v can be read fairly accurately from the -3dB or 90 degree phase point of the 40% curve. Damping can be determined from an estimate of the magnitude of the peaking present. For an under-damped second order system, the damping factor ζv can be shown to be related to peak amplitude ratio M_v in "(5)".

$$M_v = \frac{1}{2\zeta_v\sqrt{1-\zeta_v^2}} \qquad (5)$$

In this example, a reasonable estimate of peaking based on the 40% response curve would be about 1.5 dB, which corresponds to an amplitude ratio of about 1.189. A suitable value of damping determined iteratively from Equation 2 is about 0.48. Armed with these values, a simplified model of the servo-valve spool dynamics may be constructed. The input to the model will be the torque motor current derived from "(1)" normalized to the saturation current obtained from the datasheet, and the output will be the normalized spool position.

3.1.3 VALVE FLOW-PRESSURE

The servo-valve delivers a control flow proportional to the spool displacement for a constant load. For varying loads, fluid flow is also proportional to the square root of the pressure drop across the valve. Control flow, input current, and valve pressure drop are related by the following simplified equation.

$$Q_L = Q_R \cdot i_v^* \cdot x \sqrt{\frac{\Delta P_v}{\Delta P_R}} \qquad (6)$$

In "(6)", Q_L , is the hydraulic flow delivered through the load actuator, Q_R the rated valve flow at a specified pressure drop ΔP_R, and iv is normalized input current. ΔP_V is the pressure drop across the valve given by $\Delta P_V = P_S - P_T - P_L$, where P_S , P_T , and P_L are system pressure, return line tank) pressure, and load pressure respectively. Maximum power is transferred to the load when $P_L = 2/3\ P_S$, and since the most widely used supply pressure is 210 bar, it is common practice to specify rated valve flow at ΔP = 70 bar. The static relationship between valve pressure drop and load flow is often presented in manufacturer's datasheets as a family of curves of normalized control flow against normalized load pressure drop for different values of valve input current as shown in Fig. 8 [2].

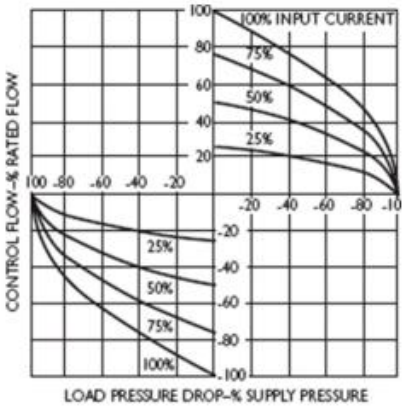

Fig. 8. Servo-valve Flow-pressure curves

The horizontal axis is the load pressure drop across the valve, normalized to 2/3 of the supply pressure. The vertical axis is output flow expressed as a percentage of the rated flow, Q_R. The valve orifice equation is applied separately for the two control ports to obtain expressions for oil flow into each of the two actuator chambers. Since load flow is defined as the flow through the load: $Q_L = Q_A = - Q_B$

A Simulink model of the servo-valve is shown in the following sections. The inputs are command voltage from the amplifier, supply and return oil pressures from the hydraulic power supply (P_S and P_T), and load pressures from the actuator chambers (P_A and P_B). Outputs are the flows to each side of the piston (Q_A and Q_B), and the load flow Q_L.

3.2 LINEAR ACTUATOR

3.2.1 CYLINDER CHAMBER PRESSURE

The relationship between valve control flow and actuator chamber pressure is important because the compressibility of the oil creates a "spring" effect in the cylinder chambers which interacts with the piston mass to give a low frequency resonance. This is present in all hydraulic systems and in many cases this abruptly limits the usable bandwidth. The effect can be modeled in "(7)" using the

flow continuity equation from fluid mechanics which relates the net flow into a container to the internal fluid volume and pressure.

$$\Sigma Q_{in} - \Sigma Q_{out} = \frac{dV}{dt} + \frac{V}{\beta}\frac{dP}{dt} \quad (7)$$

The left hand side of the equation is the net flow delivered to the chamber by the servo valve. The first term on the right hand side is the flow consumed by the changing volume caused by motion of the piston, and the second term accounts for any compliance present in the system. This is usually dominated by the compressibility of the hydraulic fluid and is common to assume that the mechanical structure is perfectly rigid and use the bulk modulus of the oil as a value for β. Mineral oils used in hydraulic control systems have a bulk modulus in the region of 1.4 x 109 N / m. Equation 7 can be re-arranged to find the instantaneous pressure in chamber A as follows:

$$P_A = \frac{\beta}{V}\int\left(Q_A - \frac{dV_A}{dt}\right)dt \quad (8)$$

3.2.2 PISTON DYNAMICS

Once the two chamber pressures are known, the net force acting on the piston (FP) can be computed by multiplying by the area of the piston annulus (AP) by the differential pressure across it as shown in "(9)".

$$F_P = (P_A + P_B)A_p \quad (9)$$

An equation of forces for piston motion can now be established by applying Newton's second law. For the purposes of this analysis, it will be assumed that the piston delivers a force to a linear spring load with stiffness K_L , which will allow us to investigate the load capacity of the actuator later. The effects of friction (F_f) between the piston and the oil seals at the annulus and end caps will also be included. The resulting force equation for the piston is shown below and may be modeled in Simulink using two integrator blocks.

$$F_p = M_p\frac{d^2x_p}{dt^2} + F_f + K_L x_p \quad (10)$$

The total frictional force depends on piston velocity, driving force F_p, oil temperature and possibly piston position. One method of modeling friction is as a function of velocity, in which the total frictional force is divided into static friction (a transient term present as the actuator begins to move), Coulomb friction (a constant force dependent only on the direction of movement), and viscous friction (a term proportional to velocity). Assuming that viscous and Coulomb friction components dominate, frictional force F_t can be modeled as in "(11)".

$$F_t = \frac{dx}{dt}F_{vo} + sign\left(\frac{dx}{dt}\right)F_{co} \quad (11)$$

Where viscous and Coulomb friction coefficients are denoted by F_{vo} and F_{co} respectively. Frictional effects are notoriously difficult to measure and accurate values of these coefficients are unlikely to be known, but order of magnitude estimates can sometimes be made from relatively simple empirical tests. One test which can yield useful information is to subject the system to a low frequency, low amplitude sinusoidal input signal, and plot the output displacement over one or two cycles. A low friction system should reproduce the input signal, but the presence of friction will tend to flatten the tops of the sine wave as the velocity falls to a level blow that necessary to overcome any inherent Coulomb friction. In actuators fitted with conventional, PTFE-based bearings, friction is related fairly linearly to supply pressure and oil temperature and care should be taken to conduct testing under representative conditions.

In a first analysis, leakage effects in the actuator are sometimes neglected, however this is an important factor which can have a significant damping influence on actuator response. Leakage occurs at the oil seals across the annulus between the two chambers and at each end cap, and is roughly proportional to the pressure difference across of the seal. Including leakage effects, the flow continuity equation for chamber A is shown in "(12)".

$$Q_A - K_{La}(P_A - P_B) - K_{Le}P_A = \frac{dV_A}{dt} + \frac{V_A}{\beta}\frac{dP_A}{dt} \quad (12)$$

where K_{La} and K_{Le} are internal and external leakage coefficients respectively. The equation for chamber B is similar with appropriate changes of sign. It is a relatively simple matter to modify the model to compute the instantaneous chamber leakages and subtract them from the total input flow.

3.3 HYDRAULIC POWER SUPPLY

The behavior of the hydraulic power supply described in Section 3.1 may be modeled in the same way as the chamber volumes: by applying the flow continuity equation to the volume of trapped oil between the pump and servo-valve. In this case, the input flow is held constant by the steady speed of the pump motor, and the volume does not change. The transformed equation is

$$P_s = \frac{\beta}{V_1}\int\left(Q_{pump} - Q_L\right)dt \quad (13)$$

Equation (13) takes into account the load flow Q_L drawn from the supply by the servo-valve, and accurately models the case of a high actuator slew rate resulting in a load flow which exceeds the flow capacity of the pump. In such cases the supply pressure P_s falls, leading to a corresponding reduction in control flow and loss of performance. The action of the pressure relief valve may be modeled using a limited integrator to clamp the system pressure to the nominal value.

4. CASE STUDY

This section presents some typical values for a high-performance, symmetrical, linear actuator. Simulation results for an actuator based on these values are shown in Fig 9,10 and 11, followed by the results of some physical tests conducted on a similar real actuator.

MODELING AND SIMULATION APPROACH

The approach of physical modeling appears to be well-suited to obtain insight in the relevant dynamic and non-linear effects of a hydraulic servo-system. In the modeling approach, the distinction of different subsystems plays an important role; it simplifies the modeling process, and it provides insight in the (dynamic) behavior of the system, caused by interaction of the subsystems. For the hydraulic servo-system this means, that a distinction is made between the servo-valve, the hydraulic actuator, and the transmission lines between the servo-valve and the actuator. In order to investigate both the dynamic properties and the non-linearities of the system, the modeling approach starts with the theoretical modeling of the subsequent subsystems. In the theoretical model, which is highly detailed, any dynamic and non-linear effect that might play a role in the hydraulic servo-system is included. By means of simulations with this model, the relevance of those effects is investigated, at least qualitatively.

Subsequent analysis of the dynamic properties of the subsystem models by means of line-arization leads to basic insight in the dynamic behavior of the hydraulic servo-system. It appears that the dynamics of the complete system can be seen as a series connection of the servo-valve dynamics and the actuator dynamics. Furthermore, in case the actuator has a long stroke, the transmission lines between the valve and the actuator compartments should explicitly be taken into account; a proper connection of the transmission line models with the basic model of the hydraulic actuator typically leads to an extended actuator model with badly damped resonances at high frequencies.

As a result of the analysis of the dynamics, a reasonably simple linear model is obtained, describing the relevant dynamic behavior of the servo-system with few model parameters, while the physical structure of the model is preserved. The latter allows including the most important non-linearities of the system in the linearized model, which have shown to be relevant by the abovementioned simulations. Thereby, only a few parameters are used to quantify the underlying non-linear physical effects, such that the simple structure of the linearized models is preserved again. In short, the most relevant non-linearities are: the torque motor non-linearity (flapper-nozzle valve dynamics), the non-linear spool port flows (the basic non-linearity of any hydraulic servo-system), Coulomb friction (if no hydrostatic bearings are applied), and position dependence of the actuator dynamics.

The linear dynamics of the system can be identified in a first step, by avoiding the excitation of the dominant non-linearity of the system during the frequency response measurement, using an input amplitude filter. This technique is especially successful for the three-stage valve with respect to the non-linearity of the pilot-valve flow. For the hydraulic actuator, the technique of input amplitude filtering is valuable to avoid too heavy excitation of the setup around the resonance frequencies of the system, while avoiding too much disturbing effect of the Coulomb friction in other frequency regions. Although for all subsystems the identified models are directly related to the underlying physical models, only the basic actuator model is sufficiently transparent to be able to reconstruct all physical parameters in the theoretical model from the identified parameters. Nevertheless, besides the basic actuator model with reconstructed parameters, the theoretical models for the transmission lines with a-priori chosen parameters also provide rather accurate predictions of the dynamic system behavior. Therefore, these models are quite useful for system design linearized model f or the servo-valve it is assumed that:

- There is no ball clearance in the pilot-valve.
- The pilot-valve spool has no Coulomb friction.
- The pilot-valve spool is critically centered and has no radial clearance.
- The main spool is critically centered and has no radial clearance

4.1 ACTUAL SYSTEM DATA

The example data presented here is based on a symmetrical, double-ended actuator with a total stroke of around 100 mm and an active piston area of around 1. Piston mass may be specified by the manufacturer, or can be calculated from a knowledge of the geometry of the actuator. For a piston of this size, a mass of around 9 Kg would be typical.

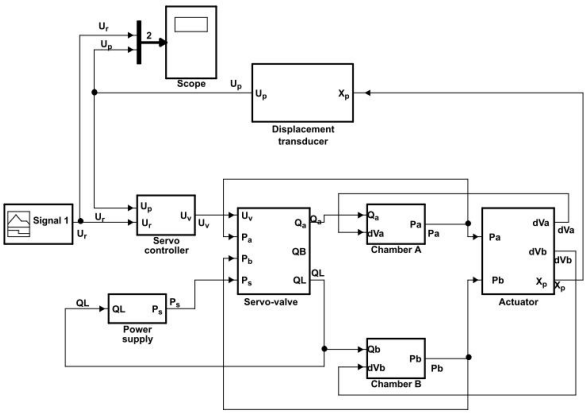

Fig. 9. Top level system diagram

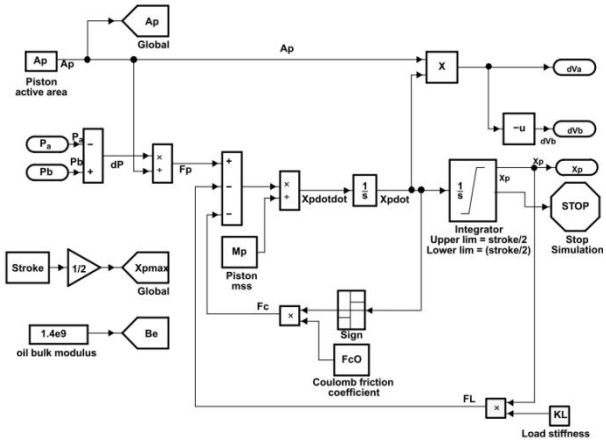

Fig. 10. Simulink Model of Hydraulic Actuator

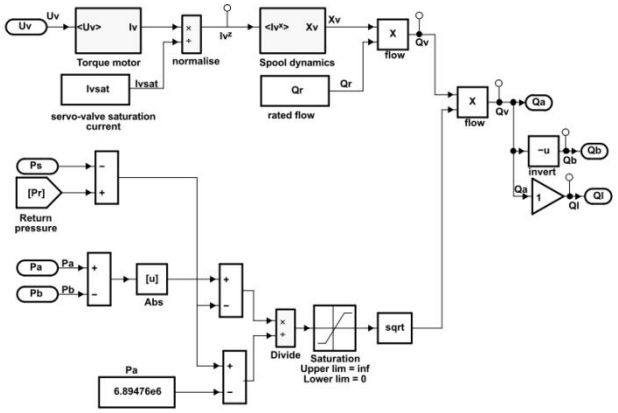

Fig. 11. Simulink Model of Servo-Valve

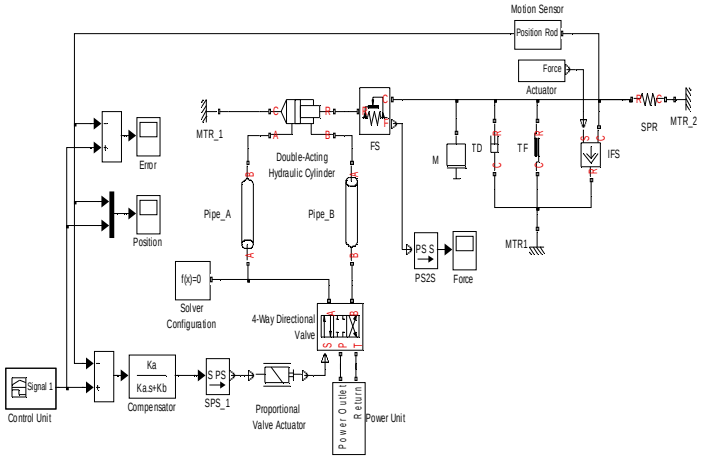

Fig. 12. Closed-Loop Electrohydraulic Actuator with Proportional Valve

TABLE 1. ACTUATOR DATA

Symbol	Description	
M_p	Mass of actuator piston	9 Kg
X_p(max)	Total stroke of the piston	0.1 m
A_p	Active area of piston annulus	645 x 10-6 m^2

Data for the servo-valve can be read directly or calculated from the manufacturer's data sheet as described in Section 4. The following values are based on the Moog 760-series valve.

TABLE 2. SERVOVALVE DATA

Symbol	Description	
Qr	Rated flow of valve at 70 bar pressure drop	0.63069 x 10-3 m3/s
Mv	Ratio of peaking in servovalve frequency response	1.5 dB
Sv	Damping ratio of servovalve model	0.48
ωv	Natural frequency of servo valve model	534 rad/s
Lc	Inductance of servovalve coil	0.59 H
Rc	Series resistance of torque motor circuit	100 Ω
Iv(sat)	Saturation current torque motor	0.02 A

The remaining data is usually available from knowledge of the system. Leakage and frictional effects could be modeled using coefficient values estimated from empirical data.

TABLE 3: MISCELLANEOUS SYSTEM DATA

Symbol	Description	
B_e	Bulk modulus of hydraulic fluid	1.4 x 10-9 N/m2
P_s	Supply pressure from the pump	2.1 x 107 Pa
P_R	Return pressure to tank	0 Pa
Q_p	Maximum flow capacity of the pump	1.67 x 10-3 m^3/s
V_t	Volume of trapped oil between pump and servo-valve	0.0005 m^3

Simulink simulation of the Closed-Loop Electrohydraulic Actuator with jProportional Valve
As shown in Fig. 12

1. Pump ramps up to speed at t = 0.2 s drops off to 25% at t = 3.5 s and then is restored at t = 7.5 s
2. The actuator consists of a proportional 4-way directional valve driving a double-acting hydraulic cylinder. The cylinder drives a load consisting of a mass, viscous and Coulomb friction, constant force, and a spring. The actuator is powered by a variable-displacement, pressure-compensated pump, driven by a constant velocity motor. Pipelines between the valve, cylinder, pump, and the tank are simulated with the Hydraulic Pipeline blocks.

4.2 SIMULATION RESULTS

A simple test which yields useful information about the performance of the system is to apply a small step signal to the input and monitor the response. In Simulink, this can be simply achieved using a 'scope' block to monitor command

and response signals. The position of the step input source and scope blocks are colored red in the system level block diagram and a typical actuator step response is shown in Fig. 13 and 14. The vertical axis is graduated in Volts measured at the error amplifier. The controller is scaled to a range of ±10V so for a 100 mm stroke actuator, a step input of +2V corresponds to a piston displacement of +10 mm from the central position.

Controller gain terms are adjusted and the step test repeated to tune the actuator response as required. The plot shown represents a satisfactory compromise between rise time and overshoot, and the corresponding controller settings would serve as a useful starting point for the control engineer when testing the real system.

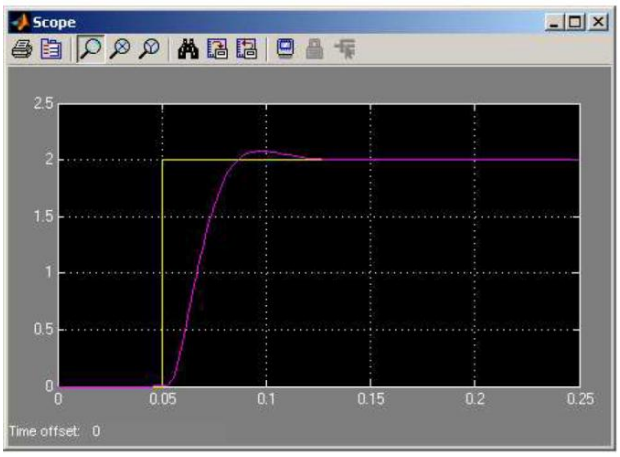

Fig. 13. Simulated Actuator Step Response

The relationship between load pressure and load flow from the servo-valve was described in Section 4.2.1. By configuring the actuator chamber pressures as test points in Simulink, a 'floating scope' block may be used to monitor these and other signals during the step response test. The graph below shows the behavior of the chamber pressures during the step response simulation. Chamber B pressure (P_B) is shown as a continuous line, and chamber A pressure (P_A) a dashed line. The vertical axis is in Pascal (N/m). The slight asymmetry results from the change in chamber volumes as the piston is displaced to its new position.

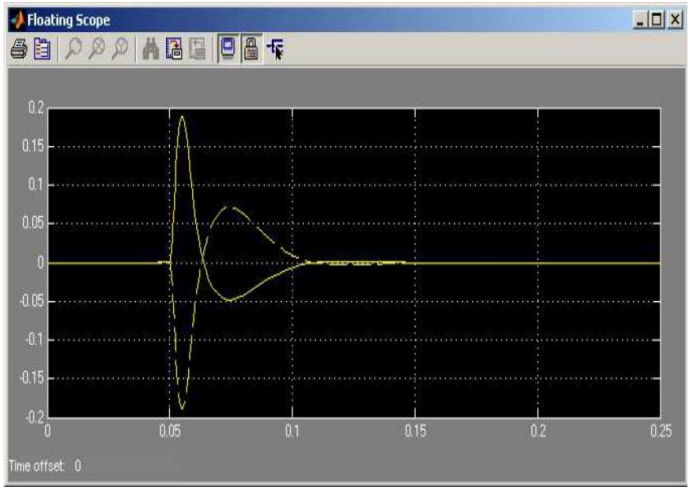

Fig. 14. Step Response of Piston Chamber Pressures

Fig. 15 shows the step response of a real high-performance linear actuator with dimensions similar to those given in Section 5.1. The sharp rising and falling edges and minimal overshoot represent the optimum response that can be obtained with a PID control strategy and a good quality actuator.

Fig. 15. Step Response of High-Performance Linear Actuator

The dynamic performance of the system is limited by the capacity of the hydraulic power supply as well as the performance of the servo-valve. This is illustrated by Fig. 16 and Fig. 17, in which a large sinusoidal command input is applied and the frequency gradually increased.

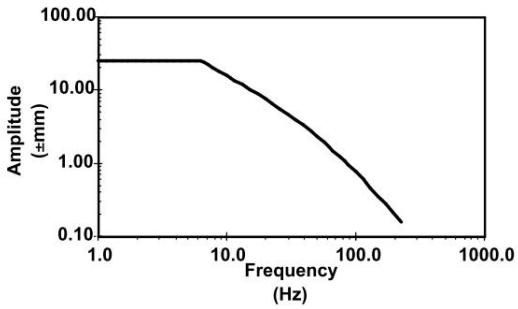

Fig. 16. Frequency Response of High-Performance Linear Actuator

The curve shows two high frequency asymptotes: the first occurs at about 8 Hz and is caused by the limited flow

capacity of the power supply. The second, at about 40 Hz, is the high frequency response limit of the servo-valve. The importance of friction in a high performance actuator is demonstrated by the following two displacement/time graphs. Both show the behavior of a linear servo-actuator when subjected to a low-frequency, low amplitude sinusoidal command input. The first shows a low friction actuator, the second actuator with higher friction caused by tighter piston and end cap oil seals.

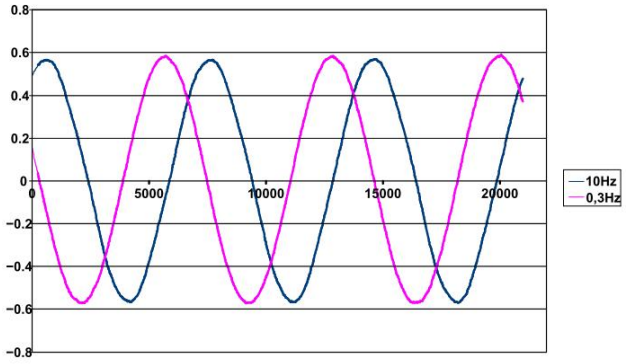

Fig. 17. Low Frequency Test on Low Friction Linear Actuator

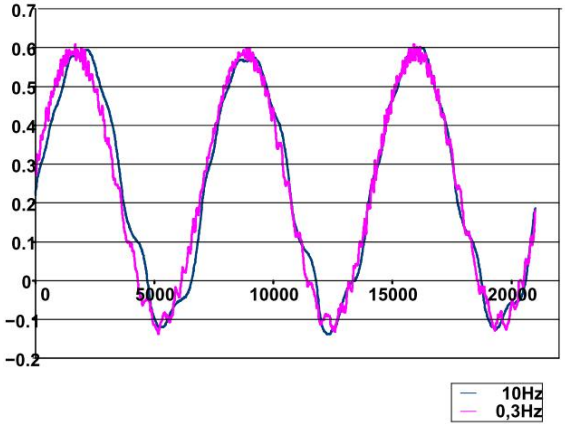

Fig. 18. Low Frequency Test on Linear Actuator with Significant Friction

Fig. 18 represents the response losses caused by friction in the actuator can be reduced to some extent by the addition of "dither" to the controller output. This is a relatively high frequency, constant amplitude oscillation, which keeps the valve spool in constant motion and reduces the break-away force needed to overcome any static friction present in the system. The use of Simulink to model and design the system allows enhancements such as this to be easily added to the digital controller.

5. CONCLUSION

This paper has examined various issues relating to the control of electro-hydraulic servo-actuators, and discussed the benefits of using digital signal processors (DSP) for digital control in these systems. A basic mathematical model has been derived based on a high performance symmetrical linear actuator, but with relatively simple parametric changes could be modified to embrace asymmetric and rotary actuator types.

The principal non-linear effects in hydraulic systems arise from the compressibility of hydraulic fluid, the complex flow properties of the servo-valve, and internal friction in the actuator. These depend on physical factors which are difficult to measure accurately and for this reason simulation results should be supported by experimental testing whenever possible.

The closed loop of electrohydraulic servovalve actuator was modeled and simulated in this article for the domain of discrete-time systems which might be use as reference in other studies in the field of hydraulic control system.

Although it is problematic to find a reasonable set of physical parameters for the theoretical servo-valve model, the preliminary simulation analysis of the model, provides a lot of insight in the non-linear dynamic behavior of the servo-valve. Dominant dynamic effects are the second order behavior of the flapper, combined with the pressure dynamics of the spool. For the three-stage valve, the dynamics are dominated by the pilot-valve dynamics at the one hand, and the integrating behavior with the feedback of the third stage at the other hand. Most important non-linearities are to be sought in the torque motor and in the flow characteristics of the pilot-valve spool and the main spool respectively.

Relatively high frequency, constant amplitude oscillation, keeps the valve spool in constant motion and reduces the break-away force needed to overcome any static friction present in the system. The use of Simulink to model and design the system allows enhancements such as this to be easily added to the digital controller

The results of this paper, being physically structured non-linear dynamic models of the hydraulic servo-system, which are sufficiently simplified to allow identification of the model parameters from experimental data, as well as experimental validation of the quality of the models.

REFERENCES

[1] M. Jelali and A. Kroll, Hydraulic Servo Systems - Modeling, Identification & Control, Springer, 2003 Moog 760 Series Servovalves, product datasheet

[2] R. H. Maskrey and W. J. Thayer, A Brief History of Electrohydraulic Servomechanisms, Moog Technical Bulletin 141, June 1978

[3] T. P. Neal, Performance Estimation for Electrohydraulic Control Systems, Moog Technical Bulletin 126, November 1974

[4] M. D'Amore and G. Pellegrinetti, Dissecting High-Performance Electrohydraulic Valves, Machine Design, April 2001

[5] D. DeRose, The Expanding Proportional and Servo Valve Marketplace, Fluid Power Journal, March/ April 2003

[6] Herbert E. Merritt, Hydraulic Control Systems, Wiley, 1967
[7] D. DeRose, Proportional and Servo Valve Technology, Fluid Power Journal, March / April 2003
[8] B. C. Kuo and F.Golnaraghi, Automatic Control Systems, Wiley, 2003
[9] J. B. Dabney and T.L. Harman, Mastering Simulink, Pearson Prentice Hall, 2004
[10] Signal Conditioning an LVDT using a TMS320F2812 digital signal processors (DSPS) (SPRA946)
[11] L. Erping and P.M. McEwan, "Analysis of a circuit breaker solenoid actuator system using the decoupled CAD-FE-integral technique,"IEEE Trans Magn., vol. 28, pp. 1279-1282, 1992.
[12] Z. Ren and A. Razek, "A strong coupled model for analysing dynamic behaviors of non-linear electromechanical systems," IEEE Trans. Magn.,vol. 30, pp. 3252-3255, 1994.
[13] L. Nowak, "Simulation of dynamics of electromagnetic driving device for comet ground penetrator. IEEE Trans. Magn., vol. 34, pp. 3146-3149, 1998.
[14] C.S. Biddlecombe, J. Simkin, A.P. Jay, J.K. Sykulski, and S. Lepaul, "Transient electromagnetic analysis coupled to electric circuits and motion," IEEE Trans. Magn., vol. 34, pp. 3182-3185, 1998.
[15] K. Srairi and M. Feliachi, "Numerical coupling models for analyzing dynamic behaviors of electromagnetic actuators," IEEE Trans. Magn.,vol. 34, pp. 3608-3611, 1998.
[16] K. Tani, T. Yamada, Y. Kawase, "Dynamic Analysis of Linear Actuator Taking into Account Eddy Currents Using Finite Element Method and 3-D Mesh Coupling Method," IEEE Trans. Magn., vol. 35, pp. 1785-1788, 1999.
[17] T. Nakagawa, K. Muramatsu, K. Koda, "Dynamic Analysis of Vacuum Interrupter with Linear Actuator," Proc. Fifth Int. Symp. on Linear Drives for Industrial Applications LDIA 2005, Kobe-Awaji, Hyogo, Japan, 2005.
[18] Espirito Santo, M.R.A. Calado, C.M.P Cabrita, "Variable Reluctance Linear Actuator Dynamics Analysis Based on Co-energy Maps for Control Optimization," Proc. Fifth Int. Symp. on Linear Drives for Industrial Applications LDIA 2005, Kobe-Awaji, Hyogo, Japan, 2005.